

GYR-TIMESCALE DESTRUCTION OF HIGH-ECCENTRICITY ASTEROIDS BY SPIN AND WHY 2006 HY51 HAS BEEN SPARED

VALERI V. MAKAROV

U.S. Naval Observatory, 3450 Massachusetts Ave., Washington, DC 20392-5420, USA

ALEXEY GOLDIN

Teza Technology, 150 N Michigan Ave, Chicago IL 60601, USA

DIMITRI VERAS

Centre for Exoplanets and Habitability, University of Warwick, Coventry CV4 7AL, UK
Department of Physics, University of Warwick, Coventry CV4 7AL, UK

Draft version July 23, 2020

ABSTRACT

Asteroids and other small celestial bodies have markedly prolate shapes, and the perturbative triaxial torques which are applied during pericenter passages in highly eccentric orbits trigger and sustain a state of chaotic rotation. Because the prograde spin rate around the principal axis of inertia is not bounded from above, it can accidentally reach the threshold value corresponding to rotational break-up. Previous investigations of this process were limited to integrations of $\sim 10^3$ orbits because of the stiff equation of motion. We present here a fast 1D simulation method to compute the evolution of this spin rate over $\sim 10^9$ orbits. We apply the method to the most eccentric solar system asteroid known, 2006 HY51 (with $e = 0.9684$), and find that for any reasonably expected shape parameters, it can never be accelerated to break-up speed. However, primordial solar system asteroids on more eccentric orbits may have already broken up from this type of rotational fission. The method also represents a promising opportunity to investigate the long-term evolution of extremely eccentric triaxial exo-asteroids ($e > 0.99$), which are thought to be common in white dwarf planetary systems.

Keywords: minor planets, asteroids: individual (2006 HY51) — celestial mechanics — methods: numerical — chaos

1. INTRODUCTION

Minor planets on highly eccentric orbits ($e \gtrsim 0.9$) play important roles during the formation and death of planetary systems. These objects contributed to the lunar bombardment (Morbidelli et al. 2018; Brasser et al. 2020) and to the accretion of primordial terrestrial planets, both within the solar system (O’Brien et al. 2018) and in extrasolar planetary systems such as TRAPPIST-1 (Dencs & Regály 2019). Around white dwarf planetary systems, highly eccentric asteroids are thought to be the primary progenitor of debris disks (Jura 2003; Debes et al. 2012; Veras et al. 2014; Malamud & Perets 2020a,b) and observed metallic pollution in the photospheres of those stars (Zuckerman et al. 2010; Koester et al. 2014).

Although often represented as point masses in numerical simulations, most known asteroids are aspherical. This asphericity significantly affects their spin dynamics, which is coupled with their orbital evolution.

The shape and distribution of mass of a rocky asteroid can be idealized and approximated with an ellipsoid with three unequal principal axes. In dynamical problems, the most important parameters of this approximation are the three corresponding moments of inertia A , B , and C , in increasing order. They can be related to the geometric

elongation parameters under the assumption of uniform density, or by direct integration for a given density profile and specific multi-layer models.

It is a well known fact that the size and mass of celestial bodies is strongly correlated with the degree of triaxiality (and, generally, with deviations from spherical symmetry), which can be represented by the dimensionless ratio $\sigma = (B - A)/C$. The benchmark value is $\sigma = 1.9 \times 10^{-5}$ for Earth (Lambeck 1980), with its mass $M_{\oplus} = 5.97 \times 10^{24}$ kg. Larger super-Earth exoplanets are likely to have shapes that are even closer to perfect spherical symmetry, while the Moon, with a mass that is roughly 100 times smaller (7.35×10^{22} kg) than Earth’s, has a more prolate shape at $\sigma = 2.28 \times 10^{-4}$. Other satellites of similar mass have even greater degrees of deformation, e.g., Io with $\sigma = 6.4 \times 10^{-3}$ (Anderson et al. 2001).

This inverse correlation between mass and σ continues into the domain of comets and asteroids, where irregular potato-like shapes are prevalent. The recently discovered asteroid ‘Oumuamua (Meech et al. 2017; Williams 2017), which is probably of interstellar origin (Higuchi & Kokubo 2019), represents an extreme case with an observable aspect ratio of 6 ± 1 (McNeill et al. 2018), which is likely to be even greater because of projection effects (Siraj & Loeb 2019).

When an elongated body in an eccentric orbit passes

close to its host¹, the former is subject to the triaxial torque of increasing magnitude due to an increasing gradient of the gravitational potential. The resulting equations of motion (Euler’s equations) have been well-established and represent three second order nonlinear differential equations, which include the instantaneous direction cosines of the longest axis and the instantaneous spin rates about all three principal axes (Danby 1962). The system simplifies into a single second order ordinary differential equation (ODE) under the assumption that the principal axis of inertia (corresponding to the moment C) is always orthogonal to the orbital plane, which nullifies the other two components of the torque and the velocity-dependent terms.

In this paper, we provide a computational method which enables long-term tracking of the spin evolution of elongated bodies on highly eccentric orbits. The 1D spin evolution model is equivalent to that in Makarov & Veras (2019). In that paper, however, evolution was computed on a timescale which is roughly six orders of magnitude shorter than the current age of the solar system. Our method enables us to support the primordial dynamical status of 2006 HY51, the asteroid whose orbit is of the highest known eccentricity.

In Section 2, we summarize our knowledge of the most eccentric solar system asteroids and provide more details about the spin evolution. We then describe our numerical integration method in Section 3, before identifying the origin of chaos in our systems in Section 4 and integrating the evolution of 2006 HY51 in Section 5. We discuss and summarize our results in Section 6.

2. THE HIGHEST ECCENTRICITY ASTEROIDS IN THE SOLAR SYSTEM

The JPL Horizons database provides a compendium of information about celestial bodies in the Solar system, which is available online². We made a selection of all Sun-orbiting asteroids in this database with semimajor axes $a < 3$ au, absolute magnitudes $H_{\text{mag}} < 20$, and eccentricities $0.95 \leq e < 1.0$ (filtering out objects on hyperbolic orbits with eccentricity above 1).

The selected 6 objects are listed in Table 1. They do not appear to have attracted much attention in the literature, except as representing potentially hazardous Near-Earth Objects. Although these objects are usually faint with visual magnitudes in the 23–25 range, they become bright during brief perihelion flybys. The most eccentric orbit is found for 2006 HY51, which is arguably the most studied object on the list. It is the only one with an estimated diameter, which is 1.218 km. Its rate of rotation is unknown.

These six asteroids of the Apollo group have approached the Sun within 0.1 au every 3 or 4 years over most of the solar system’s lifetime (billions of years). The spin of these objects, driven by the periodic flybys, is chaotic. Chaotic rotation of prolate asteroids is predicted theoretically (Wisdom et al. 1984), as well as observed in the solar system (Kouprianov & Shevchenko 2005). Even if some of the currently synchronized planetary satellites of elongated shape, such as Phobos and

Epimetheus, stay within an island of stable libration, they could not have reached this state without crossing a zone of chaotic motion in the past (Wisdom 1987).

Minor bodies in highly eccentric orbits, on the other hand, are permanently in the chaotic state of rotation driven by the impulsive kicks during brief periapse phases (Makarov & Veras 2019). The rate of rotation around the principal axis of inertia is a continuous function of time with step-like changes, which can be considered as a random process when discretized at apoastron times.

At a given apoastron rotation velocity, as demonstrated with direct numerical integrations, the distribution of velocity updates is a concave function of the orientation angle. This distribution is also biased with respect to zero in such a way that the greatest positive updates are larger in absolute value than the greatest negative updates at small and moderate apoastron spin rates, and the opposite bias is present for high prograde spin rates. This curious property makes the chaotic evolution weakly stationary and self-regulating, so that if the spin rate stochastically becomes very high, the updates are more likely to reduce it. Even though the velocity is not bound on the high end, the regulation mechanism may require a long time for the process to reach the break-up spin, depending mostly on orbital eccentricity.

This property of the long-term evolution of the regulation mechanism is the primary motivation for this work. Although rotational break-up over just 10^3 orbits has been invoked to generate the ring of debris material orbiting white dwarf ZTF J0139+5245 (Vanderbosch et al. 2019; Veras et al. 2020), the short timescale chosen for the integrations restricted the parameter space which could be explored. Integrations which last over the lifetime of the solar system now allows us to probe the evolution of solar system asteroids like 2006 HY51 and help assess if they could be primordial.

3. NUMERICAL INTEGRATION OF MOTION

We adopt the 1D model described in Makarov & Veras (2019), which uses a simplified equation of motion with the axis of rotation aligned with the principal inertia axis C and orthogonal to the orbital plane at all times. The torque acting on the asteroid is then parallel to C . This assumption is realistic when the asteroid is spinning fast in the prograde sense so that its angular momentum is aligned with the orbital angular momentum, and free librations around the other axes of inertia can be ignored. We performed limited integrations (which are much more computer-intensive) of the full triaxial equation of motion with random initial conditions. These simulations confirmed that the principal axis rotation remains strongly chaotic and driven by impulse-like interactions at perihelia. We surmise that the time scale of spin evolution may become somewhat longer due to the geometric projection of the longest axis at nonzero inclination, but this needs to be confirmed by extensive computer modelling.

The sidereal orientation angle θ in the equatorial plane of the asteroid is convenient to measure from the direction to the perturber’s periapse (perihelion in our case) and the longest axis of the ellipsoid A . A second-order ODE includes θ , its first time derivative $\dot{\theta} = \omega$, and its second time derivative (rotational acceleration), as well as the triaxiality parameter $(B - A)/C \equiv \sigma$, the orbital

¹ If the elongated body is an asteroid or comet, the host is the parent star. The elongated body may also be a satellite, in which case the host is the parent planet.

² <https://ssd.jpl.nasa.gov/?horizons>

Table 1
High-eccentricity asteroids.

Name	e	a au	r_{\min} au	P_{orb} yr
394130 (2006 HY51)	0.9684	2.590	0.082	4.17
(2011 KE)	0.9546	2.206	0.100	3.28
465402 (2008 HW1)	0.9600	2.586	0.103	4.16
(2012 US68)	0.9579	2.504	0.105	3.96
399457 (2002 PD43)	0.9560	2.508	0.110	3.97
431760 (2008 HE)	0.9505	2.261	0.112	3.40

mean motion n , the semimajor axis a , the instantaneous orbital distance r , and the true anomaly f . Two initial conditions are arbitrarily chosen at times $t = 0$ for both θ and ω . These conditions are sufficient to integrate this equation in time and to determine the functions $\theta(t)$ and $\omega(t)$. We further compute the true anomaly from the mean anomaly and the eccentric anomaly, which is also needed to compute r , via Kepler’s equation and reverse interpolation.

This integration requires special care for high values of eccentricity because of rapid, large amplitude variations of the integrated parameters at short perihelion passages, where the polar torque suddenly increases by several orders of magnitude. This problem is therefore stiff, requiring that the integration algorithm adopt an un-economical very small integration time step, or adjust the integration step according to the local stiffness.

Integration of the ODE with the parameter values for 2006 HY51 (listed in Table 2) confirms that the principal axis rotation of this object is strongly chaotic because of abrupt changes of ω at perihelia of seemingly random magnitudes and direction. If we only record the values of $\omega = \theta$ at the times of aphelia, then the stochastic changes of this parameter – an example of which is shown in Fig. 1 – can be formally fitted as a discrete random process, similar to a random walk.

These fits using general random process models are not very successful because they do not capture peculiar properties of the stochastic behaviour (Makarov & Veras 2019). Specifically, the velocity differences or “updates” between consecutive aphelion passages, $d_{\omega,i} = \omega_i - \omega_{i-1}$, for a fixed ω_{i-1} , do not follow a Gaussian distribution, or even a bell-shaped distribution. The spin updates $d_{\omega,i}$ in Fig. 1 are relatively small, resulting in a fairly slow variation of the spin rate, because of the strong statistical dependence of this parameter on the spin rate itself.

We performed a series of exact long-term integrations (which are much slower than our new method) of 9000 orbits each for 2006 HY51 with different initial parameters and recorded the tuples $\{\omega_{i-1}, d_{\omega,i}\}$ for each orbit. The result of one such exact integration is shown in Fig. 2. Each dot represents one aphelion tuple. The occupied area in the parameter space is similar in shape to the distributions found for exo-asteroids orbiting white dwarfs at higher eccentricity (Makarov & Veras 2019). The range of possible updates at a fixed aphelion velocity is finite with sharp boundaries, which are not symmetric around zero. The upper boundary of positive updates is markedly greater in absolute value than the lower boundary for negative updates at $\omega \lesssim 100 n$. Therefore, the spin rate will not stay in this low-value regime for a long

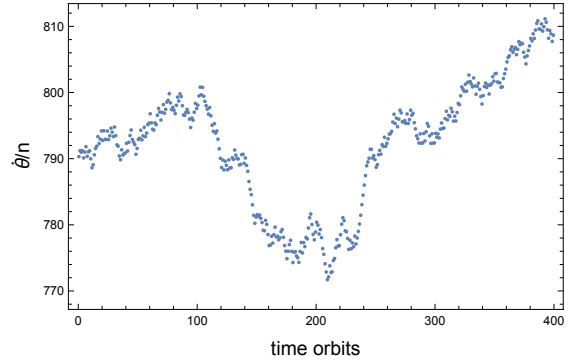


Figure 1. Simulation of spin rate in units of mean motion of the 2006 HY51 asteroid for 400 consecutive orbits by small time-step integration with stiffness switching. Only the aphelion values of rotation rate are shown with dots.

time and inevitably will meander to higher values. The opposite asymmetry is found at $\omega \gtrsim 200 n$, and although ω is not bounded on the high end, the general trend is to stochastically slow down.

This peculiar probability distribution of velocity updates makes the process somewhat self-regulated. In the context of this study, we are interested in the high spin regime of the process. What is the likelihood of the spin rate achieving very high prograde values?

The narrow funnel at the high end of the distribution stretches to infinity (Fig. 2), but the range of possible updates also infinitely decreases, maintaining a tiny negative bias. Therefore, when the spin rate becomes higher than several hundred n , the updates will be small and the asteroid will become stuck in this area for an extended interval of time, with the probability of spinning further up becoming negligibly small. Indeed, this specific realization failed to reach spin rates much above $700 n$ in 9000 orbits. Given a much longer time, it is a matter of probabilities that the spin rate increases to, say, $1000 n$. We hence would like to answer these questions: how likely is it for 2006 HY51 to reach the fission threshold within a certain time span; or, alternatively, what is the characteristic time of reaching the fission velocity at a certain probability?

Although these questions can be answered through expensive numerical simulations, such direct in-orbit integrations are too computer-intensive and slow. The limited integrations presented in Figs. 1 and 2 indicate that it may be impossible for 2006 HY51 to ever reach the fission velocity within the solar system age. To confirm and verify this surmise, we look for a surrogate simulation model representing this stochastic process. The idea is to compute the velocity update $d_{\omega,i}$ directly from tuples $\{\theta_{i-1}, \omega_{i-1}\}$ for each orbit avoiding the in-orbit

Table 2
Observed and assumed parameters of 2006 HY51.

Parameter	Value	Unit	Origin
Period, P_{orb}	4.17	yr	observed
Mean motion, n	0.00413	rad d ⁻¹	observed
Semimajor axis, a	2.59	au	observed
Eccentricity, e	0.9684		observed
Mass, M_2	7.6×10^9	kg	assumed
Radius, R	0.609×10^3	m	observed
Triaxiality, $\sigma = (B - A)/C$	0.2		assumed

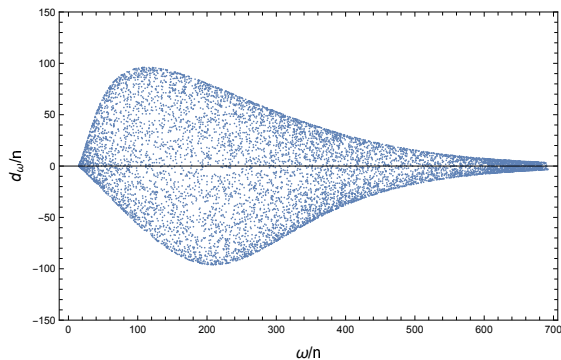


Figure 2. Spin rate updates versus spin rates at aphelion for 50 000 numerically integrated orbits of 2006 HY51 with $\sigma = 0.2$. Integration of the equation of motion.

4. THE ORIGIN OF CHAOS

We consider the function $d_\omega(\theta, \omega)$ (herewith we drop the indices for brevity) and its properties. This function is deterministic, i.e., given a pair of specific aphelion parameters, it takes one exact value, which can be accurately computed. This feature may seem to contradict the obviously chaotic character of the process, but the model function does not have to be stochastic for chaos to emerge. For example, the function may have discontinuities or singularities, but not for asteroid rotation (at least, when the parameters are not too close to a separatrix).

Fig. 3 shows the function values computed by full-scale integration for a fixed aphelion velocity $\omega = 200n$ and a grid of orientation angles θ covering the entire range $[0, \pi]$. The function is a remarkably smooth and simple periodic function with two dominating harmonics $\sin 2\theta$ and $\sin 4\theta$, and a constant term. Interpretation of this function is intuitively clear: at a fixed aphelion velocity, the object rotates almost uniformly on the way to perihelion because the torque is numerically small at a great distance from the Sun until it reaches the point of perihelion, where the violent interaction takes place within a very short interval of time. The object will make a certain number of revolutions between the aphelion and perihelion, which is weakly dependent on the initial orientation angle. But the outcome of the perihelion interaction is strongly (almost exclusively) dependent on the orientation angle at perihelion. By changing the aphelion θ we change the perihelion θ by nearly the same amount, and variation in θ within 1π samples the entire range of possible velocity updates.

In another experiment, we fix the aphelion angle at a certain value and change the aphelion velocity ω in the vicinity of the initial $\omega_0 = 200n$. Numerical integrations

confirm that *nearly* the same range of d_ω is sampled when ω varies within $[-1/2n, +1/2n] + \omega_0$. Furthermore, the curve $d_\omega(\omega)$ looks remarkably similar to the dependence $d_\omega(\theta)$ on these intervals, apart from an additional slow trend in the former. The reason for this similarity is that the two effects are interchangeable, i.e., the same value of perihelion orientation can be achieved by either adjusting the aphelion orientation within π or by adjusting the aphelion velocity within $1n$.

We can accurately map the 2D function $d_\omega(\theta, \omega)$ on a grid of points covering the domain of interest, which is between the minimum “stop” velocity ($\simeq 20n$, according to Fig. 2) and the fission critical velocity, and 0 to π in angle. This function takes high-frequency wiggles in the ω dimension, but is smooth and sinusoid-like along θ almost everywhere, except in the corner close to the minimum velocity. We speculate that in that area of the parameter space, the system has to cross the separatrix to probe very slow prograde or retrograde velocities.

Where does the explicitly chaotic behaviour come from in this system with a smooth and integrable model function? The cause of chaos in this case is the large sensitivity of the aphelion angle to the preceding perihelion velocity update. The asteroid makes multiple rotations on each half-orbit, to the effect that even a small change in ω can sample the entire range of θ . Therefore, the velocity update at each perihelion becomes almost independent of the previous perihelion configuration and the previous velocity update. This explains why the sequence $d_{\omega,i}$ is best approximated with a GARCH(1,1) random process with the current variance strongly dependent on the preceding variance but weakly dependent on the preceding value (Makarov & Veras 2019). There is no obvious correlation with the state just two orbits ago, because the aphelion orientation angle is effectively scrambled at each periastron passage.

5. LONG-TERM SIMULATIONS OF 2006 HY51

The smoothness of the model function $d_\omega(\theta, \omega)$ opens up the possibility to replace the cumbersome small-step integration of the equation of motion with a very fast and efficient simulation of tuples $\{\omega_{i-1}, d_{\omega,i}\}$. We replace this function with a 2D interpolation function defined on a grid of points in a rectangular area in the $\{\theta, \omega\}$ plane.

Fig. 4 shows such an interpolation function computed on a grid of nodes separated by $\pi/10$ in θ and $20n$ in ω . This function is very smooth everywhere except in the close vicinity of the lower bound of velocity. It does not, however, capture the waves between the interpolation nodes in the ω dimension, which have a period of $1n$. We will explain now why this smoothed version of the

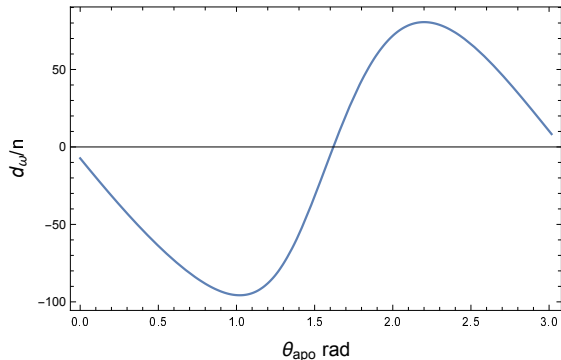


Figure 3. Spin rate update d_ω/n as a function of aphelion orientation angle θ_{apo} at a fixed aphelion spin rate $\omega_{\text{apo}}/n = 200$.

model function is sufficient for accurate simulation of the rotation process.

As we discussed in Sect. 4, the process of rotation at high eccentricity is almost memory-less, in that each aphelion orientation is barely correlated with the previous aphelion state. Therefore, without a loss of fidelity, the aphelion orientation θ can be randomized, i.e., drawn from a uniform distribution over $[0, \pi]$ at each orbit. The simulation process starts with some initial values $\{\theta_1, \omega_1\}$ and the corresponding d_ω is computed from the interpolation function shown in Fig. 4. The next state is computed simply as $\omega_2 = \omega_1 + d_\omega$, while θ_2 is a random number between 0 and π . This randomization of θ makes it unnecessary to take into account for the 20 waves of the actual model function between the nodes, because the computed d_ω values are drawn from the same distribution while the interpolation function accurately captures the smooth part of the velocity-dependent variation.

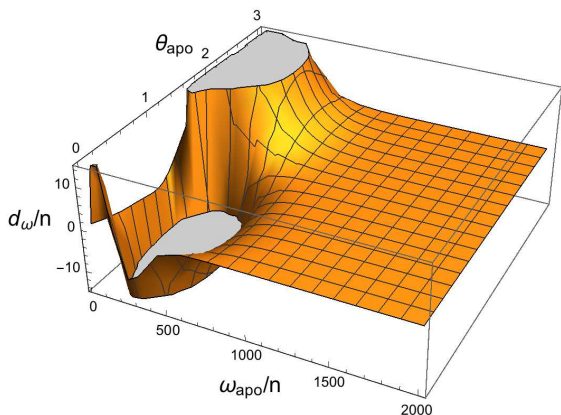


Figure 4. Interpolation function of spin rate updates $d_\omega(\omega_{\text{apo}}, \theta_{\text{apo}})/n$ estimated from grid integration. The extrema of the function are clipped to better show the complex behavior at the lower boundary of spin rate, $\omega_{\text{apo}}/n \simeq 20$.

By using this fast simulation method, we performed 100 Monte-Carlo simulations of rotation of the 2006 HY51 for 5×10^6 orbits each, with the parameters listed in Table 2. This ensemble is practically equivalent to a single simulation of 5×10^8 orbits, or 2.085 Gyr, because the initial conditions for each trial can be arbitrarily chosen. One of the simulated rotation curves is shown in Fig. 5. The spin rate rarely increases beyond $700n$, where the range of possible updates shrinks almost to zero. The highest spin rate at aphelion achieved in this

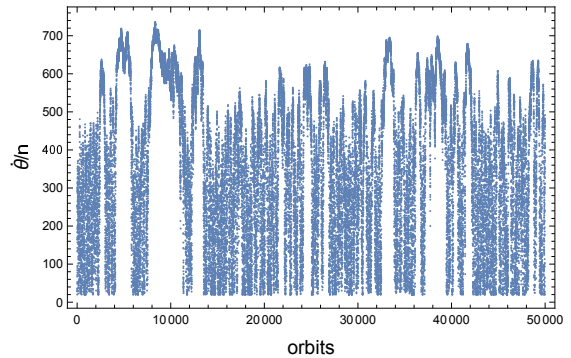


Figure 5. Chaotic evolution of the 2008 HY51 asteroid rotation rate simulated using our fast Monte-Carlo method. Only a small section of 50000 orbits from a much longer integration span is shown.

simulation is $994n$, which corresponds to a period of 1.5 d. The median spin rate over half a billion orbits is $369n$ ($P_{\text{rot}} = 4.1$ d).

The unknown parameter σ , which defines the prolate shape of the asteroid, has the highest significance for rotation evolution. In the previous set of trials, $\sigma = 0.2$ has been used. To estimate the potential uncertainty in σ , we performed a similar set of trials with $\sigma = 0.4$. Exact integration for a much smaller duration showed that approximately twice as large velocity updates are possible, as expected, and that the asymmetry of the distribution presented in Fig. 2 is much more pronounced. More importantly for this study, the high-velocity funnel is wider than in the $\sigma = 0.2$ case. We should expect higher spin rates being achieved more easily. However, the long-term simulations with the fast method reveal that the gain is rather modest. The median velocity is $419n$ ($P_{\text{rot}} = 3.6$ d), and the absolute maximum is $1035n$ ($P_{\text{rot}} = 1.5$ d).

6. SPIN-ORBIT RESONANCES

To validate the results obtained with our fast tuple simulation method with random aphelion orientations, we performed multiple, long-term simulations with a high fidelity algorithm which requires massive computations on parallel computer cores. This modification³ is based on a re-parameterization of the problem introducing an auxiliary parameter $\theta^* = \theta_{\text{ap}} + \pi \omega_{\text{ap}}/n$, which is numerically close to, but better behaved, than the actual value of θ at perihelion. An interpolation function $d_\omega(\theta^*, \omega)$ is computed on a fine grid of nodes in both arguments. The main advantage of this re-parameterization is a much smoother interpolation function $\theta(\omega, \theta^*)$ without the high-frequency waves in the ω dimension. Using the new $\theta_{\text{ap}}(\omega, \theta^*)$ function in addition to $d_\omega(\theta^*, \omega)$ allows us to compute both the velocity update and the next aphelion orientation angle for each orbit without replacing θ_{ap} with a randomly generated number. The downside of this method, besides its higher computing requirements, is that the interpolation functions become shredded at the low- ω boundary, resulting in occasional “diffusion” into the range of retrograde spins – a process we never saw in our limited full-scale integrations.

With this high-fidelity algorithm, we performed 512 simulations of the spin rate process each covering 250

³ Our simulation code in Julia for this modification of rotation simulation method is available online at <https://github.com/agoldin/2006HY51>

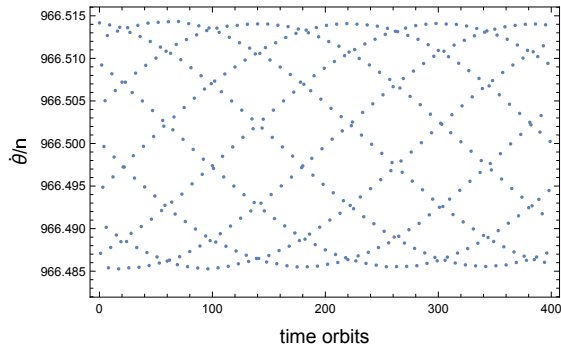


Figure 6. Resonance rotation of the 2008 HY51 asteroid simulated with full-scale integration of the equation of motion. Only aphelion values of spin rate are shown. The initial parameters were found using long-term simulations with the high-fidelity interpolation technique (see text).

million orbits. The overall behaviour and statistics of these simulations are in excellent agreement with the fast Monte-Carlo method, with one important difference. Only a small fraction of these trials demonstrated chaotic walk through the end of the time span. The rest ended up in certain quantum states in the parameter space characterized by nearly constant aphelion orientations and spin rates. These are spin-orbit resonances similar to the “islands” of stable rotation found by Wisdom et al. (1984), but pushed to the domain of very high velocities. We can estimate the characteristic time of capture into resonance by counting the quantiles of the chaotic phase durations. Of the entire set of 512 simulations with random initial conditions, 25% were captured within $2.5 \cdot 10^6$ orbits, and 50% – within $6.5 \cdot 10^6$ orbits. Thus, a significant fraction of trials show resonance capture within 20 to 50 million years. The resonance endpoints in ω_{ap}/n are quantized with the lowest frequency around 960. We note that the resonance spin rates are only slightly lower than the maximum values seen at the chaotic stages. The aphelion orientation angles are integer multiples of $\pi/2$.

We verified these results by taking one of the endpoints with $\theta_{\text{ap}} = 4.71115727$ rad, $\omega_{\text{ap}} = 966.514171$ n (with $n = 0.00412528$ rad d^{-1} , $\sigma = 0.2$, $e = 0.9684$) and used it as initial condition in numerical integration of 400 orbits. The output is depicted in Fig. 6. The trajectory is periodic circulation around a point of stable equilibrium with ω varying within a narrow range. Only one force is in action in the system, and it may seem puzzling how this resonance can be stable in the absence of a restoring force. We found a semi-qualitative interpretation, which also explains why the resonances are limited to the range of extreme rotation velocities.

The function $d_{\omega}(\theta, \omega)$ considered in §5 has multiple roots. Replacing aphelion θ and ω with x and y for convenience, the differential updates to these parameters are $\{dx, dy\} = f(x, y)$. The roots of f form lines in the $\{x, y\}$ plane, which are spaced by roughly 1 n in the frequency dimension. When during the chaotic walk in the parameter space the process hits one of the roots $\{x_0, y_0\}$, the updates are nullified and the process becomes constant. For this state to be stable, a small departure from the exact root value δ should result in an opposite-signed update, which should be smaller in absolute value than 2δ . We know that at high prograde rates the function is approximately sinusoidal so we can write at fixed $x = x_0$ that $dy'(x_0, y_0 + \delta) = \Omega \sin(2\pi\delta/n)$. Using the first-order

Taylor expansion in δ , $dy' = 2\pi\Omega \delta/n$ with a plus or minus sign for the two roots in x . Only the root with a minus sign is of interest, and the condition of stability is then

$$\Omega < n/\pi \quad (1)$$

We know from our numerical integrations that the amplitude of possible velocity updates becomes that small only at high prograde rates of rotation (cf. Fig. 2). The limiting aphelion rate is approximately 960 n . Multiple roots exist at lower rates but these equilibria are inherently unstable because the updates are greater than the perturbation.

7. DISCUSSION AND CONCLUSIONS

We have presented a fast method to compute the long-term spin evolution of triaxial asteroids on highly eccentric ($e > 0.9$) orbits around stars, or, equivalently, highly eccentric triaxial satellites around planets. The method relies on computing the velocity update after each pericenter passage – not through direct numerical integration, but rather with a surrogate function which accurately mimics the stochastic time evolution. This deterministic function $d_{\omega}(\theta, \omega)$ is usually smooth (Fig. 3), enabling one to create an interpolation function for the integration (Fig. 4).

We used the method to study the spin evolution of 2006 HY51 – the asteroid with the highest known orbital eccentricity ($e = 0.9684$) – over 2 Gyr, and found that it does not spin itself apart. The maximum spin rates seen in Gyr-long simulations are an order of magnitude lower than the estimated fission threshold, which corresponds to $P_{\text{rot}} \simeq 3$ hr (Veras et al. 2020). Our simulations did not include the possibility of chance encounters with Mercury, Venus, Earth or Mars during the 2 Gyr evolution of 2006 HY51. Even if a close encounter did occur, any changes to the rotation speed of the asteroid would be small and quick, and those types of perturbations will not likely trigger a sequence of spin updates leading to breakup.

Our result suggests that (i) no other asteroids currently seen in the solar system are in danger of radiation-less rotational fission within the age of the solar system, and that (ii) the epoch when the asteroids achieved their current orbits cannot be constrained by considering this type of breakup. However, primordial asteroids with eccentricities higher than that of 2006 HY51 could have broken up and no longer be visible. In principle, for a given population and migration model of the early solar system (Nesvorný 2018), the population of minor planets perturbed onto highly eccentric orbits can be time-evolved with our method to determine the fraction which break up, and the timescale for doing so.

This study also confirms that the chaotic rotation of small-impact parameter asteroids in Table 1 is subject to abrupt changes at perihelion passages, which should be measurable. The median spin period of the 2006 HY51, as follows from our long-term simulations, is 3 – 4 d, but it may take any values in a very wide range with periods as short as 1.5 d. If the period is close to this median value today, the next perihelion passage may result in a jump of up to 0.7 d in spin period. It would be important to observe this update to verify the prediction. The required determination of the spin period before and after

the nearest perihelion may be challenging, however, due to the faintness of these objects. They become bright only for a few weeks or even days when they are close to the Sun, both geometrically and in the sky projection, which precludes ground-based observations. For example, the 2012 US68 asteroid, which is about 22 mag at the time of writing this paper, will become as bright as 17.6 mag on 2020-May-12, and will be brighter than 18 mag for some 25 days around this date, but it will also be close to the lower conjunction with the Sun. Thus, the light curves of these objects can be determined only when they are far away from the perihelion, and hence are faint.

For triaxial moons in our solar system, rotational breakup would not be a consideration: all known moons have orbital eccentricities less than that of Nereid ($e \approx 0.75$). Nevertheless, our method might be useful to track the time evolution of moons which feature chaotic spin evolution (Tarnopolski 2017a,b). Further, the as-yet-undetermined population of exo-moons might provide additional candidates which are suitable for application with our tool.

We discovered the existence of stable spin-orbit resonances at high prograde rates of rotation in the simplified 1D model with a single polar torque component. In multiple simulations with a high-fidelity simulation technique, 2006 HY51 is captured with a probability of 0.5 into one of such resonances within 6.5 Myr, at which point chaotic evolution of rotation ceases and a periodic, small-scale circulation begins. This find does not obviate the main conclusion that 2006 HY51 and similar asteroids in high eccentricity orbits cannot be destroyed by spin, because the resonances are still an order of magnitude short of the break-up velocity. It is on our to do list to investigate if the fascinating high-spin resonances are still possible in the more realistic 3D regime when the obliquity is nonzero and all three principal axes torques are engaged. Furthermore, even a small perturbation from interaction with one of the inner planets can possibly remove the asteroid from resonance, for it to start on another chaotic journey for millions of years.

Finally, our method for fast evolution may have important implications for white dwarf planetary systems, where a variety of dynamical scenarios can perturb asteroids onto orbits with $e > 0.99$ (Veras 2016) with observable consequences (Jura & Young 2014; Vanderburg et al. 2015; Farihi 2016; Doyle et al. 2019; Vanderbosch et al. 2019; Manser et al. 2020). The maximum pericenter at which rotational breakup could occur was estimated to be about 0.015 au (Veras et al. 2020), but that value was based on full integrations over just 10^2 orbits. A comprehensive parameter space study with our fast integration method over $\sim 10^9$ orbits might reveal that this maximum pericenter is much greater.

Even if 0.015 au is taken as the tentative limiting value, one may compare it with the orbital pericenter of 2006 HY51, which is 0.082 au. The gap between these two values is sizeable, and where the transitional value for destruction lies in-between is unknown. However, sublimation effects from the Sun would extend further than those from typical white dwarfs, suggesting that this pericenter difference may not solely be due to fundamental properties of chaotic spin evolution. A search in the Horizons

database for all asteroids with a closest perihelion distance $r_{\min} < 0.085$ but without a brightness limit reveals several more poorly known asteroids in the main belt in somewhat closer orbits, with an apparent cutoff at $r_{\min} = 0.07$ au. These objects have shorter orbital periods than the 2006 HY51, with the closest orbit for the 2005 HC4 : $P = 2.46$ yr, $r_{\min} = 0.071$ au, $a = 1.823$ au, $e = 0.9613$. If we also select comets with the same search criteria, 23 additional objects emerge with perihelion separations much shorter than 0.07 au. Interestingly, there is an inverse correlation between r_{\min} and the orbital period in this sample, with the closest ‘‘Sun-grazing’’ comets having periods of hundreds of years. For example, the comet Pereyra (C1963 R1) has $P = 903$ yr and $r_{\min} = 0.005$ au, probably the closest perihelion in the Solar system. A much longer period implies a much slower chaotic evolution of rotation velocity; still, our analysis indicates that such extreme comets may be transient and short-lived.

ACKNOWLEDGMENTS

DV gratefully acknowledges the support of the STFC via an Ernest Rutherford Fellowship (grant ST/P003850/1).

REFERENCES

- Anderson, J. D., et al. 2001, *J. of Geophys. Res.*, 106, 32963
 Brasser, R., Werner, S. C., & Mojszsis, S. J. 2020, *Icarus*, 338, 113514
 Danby, J.M.A. 1962. *Fundamentals of Celestial Mechanics*. MacMillan, New York
 Debes, J. H., Walsh, K. J., & Stark, C. 2012, *ApJ*, 747, 148
 Dencs, Z., & Regály, Z. 2019, *MNRAS*, 487, 2191
 Doyle, A. E., Young, E. D., Klein, B., et al. 2019, *Science*, 366, 356
 Farihi, J. 2016, *New Astronomy Reviews*, 71, 9
 Higuchi, A., Kokubo, E. 2019, arXiv:1911.04524
 Jura, M., & Young, E. D. 2014, *Annual Review of Earth and Planetary Sciences*, 42, 45
 Jura, M. 2003, *ApJL*, 584, L91
 Koester, D., Gänsicke, B. T., & Farihi, J. 2014, *A&A*, 566, A34
 Kouprianov, V. V., & Shevchenko, I. I. 2005, *Icarus*, 176, 224
 Lambeck K. 1980. *The Earth’s variable rotation*. Cambridge University Press, New York
 Makarov, V.V., Veras, D. 2019, *ApJ*, 886, 127
 Malamud, U., & Perets, H. B. 2020a, *MNRAS*, 492, 5561
 Malamud, U., & Perets, H. B. 2020b, *MNRAS*, In Press, arXiv:1911.12184
 Manser, C. J., Gänsicke, B. T., Gentile Fusillo, N. P., et al. 2020, *MNRAS*, 493, 2127
 McNeill, A., Trilling, D. E., Mommert, M. 2018, *ApJ*, 581, L1
 Meech, K. J., Weryk, R., Micheli, M., et al. 2017, *Nature*, 552, 378
 Morbidelli, A., Nesvorný, D., Laurenz, V., et al. 2018, *Icarus*, 305, 262
 Nesvorný, D. 2018, *ARA&A*, 56, 137
 O’Brien, D. P., Izidoro, A., Jacobson, S. A., et al. 2018, *Space Science Reviews*, 214, 47
 Siraj, A. & Loeb, A. 2019, *RNAAS*, 3, 15
 Tarnopolski, M. 2017a, *A&A*, 606, A43
 Tarnopolski, M. 2017b, *Celestial Mechanics and Dynamical Astronomy*, 127, 121
 Vanderbosch, Z., Hermes, J. J., Dennihy, E., et al. 2019, Submitted to *ApJL*, arXiv:1908.09839
 Vanderburg, A., Johnson, J. A., Rappaport, S., et al. 2015, *Nature*, 526, 546
 Veras, D., Leinhardt, Z. M., Bonsor, A., Gänsicke, B. T. 2014a, *MNRAS*, 445, 2244
 Veras, D. 2016, *Royal Society Open Science*, 3, 150571
 Veras, D., McDonald, C.H., Makarov, V.V. 2020, *MNRAS*, 492, 5291

- Vokrouhlický, D., Breiter, S., Nesvorný, D., Bottke, W.F. 2007, *Icarus*, 191, 636
- Williams, G. 2017, MPEC, 2017-U181: : Comet C/2017 U1 (PanStarrs). IAU Minor Planet Center
<https://www.minorplanetcenter.net/mpec/K17/K17UI1.html>
- Wisdom, J., Peale, S. J., Mignard, F. 1984, *Icarus*, 58, 137
- Wisdom, J. 1987, *AJ*, 94, 1350
- Zuckerman, B., Melis, C., Klein, B., Koester, D., & Jura, M. 2010, *ApJ*, 722, 725